Analytical Methods

ROYAL SOCIETY OF CHEMISTRY

PAPER

View Article Online
View Journal | View Issue

Cite this: *Anal. Methods*, 2026, **18**, 1626

A novel approach for discriminating lipophilic bisphosphonate-based pharmaceuticals using a potentiometric array

Tatiana V. Shishkanova, *[a] Annemarie Skálová-Coufal, [a] Jaroslav Otta, [b] Martin Člupek [a] and Martin Vrňata [b]

Bisphosphonates are pharmaceutical compounds commonly used in the treatment of osteoporosis, Paget's disease, and multiple myeloma. Their lipophilicity was evaluated using a sensor array composed of poly(vinyl chloride) (PVC)-based ion-selective membranes (ISMs), modified with a polyaniline (PANI) layer that affects surface properties and acts as an anion-exchanger. The lipophilicity of bisphosphonates including ibandronate, clodronate, risedronate, and alendronate was analyzed in both standard and commercial samples. The influence of membrane composition (presence or absence of an anion-exchanger) and PANI deposition conditions (monomer form and/or salt content) on membrane surface properties (lipophilicity and signal stability) was investigated and confirmed using surface-wetting characterization, SEM-EDS mapping and potentiometry. Principal component analysis (PCA) enabled discrimination among the bisphosphonates based on their lipophilicity and revealed distinct contributions of individual ISMs in both standard and commercial samples.

Received 1st October 2025
Accepted 2nd February 2026

DOI: 10.1039/d5ay01639h

rsc.li/methods

1. Introduction

Lipophilicity is a fundamental physicochemical property that contributes to the absorption, distribution, metabolism, excretion, and toxicity of the pharmaceuticals. This parameter affects the solubility and permeability of pharmaceuticals, which in turn influence their potency and selectivity. It is therefore essential to monitor and consider the lipophilic properties of pharmaceuticals during their development in order to improve quality and enhance the likelihood of therapeutic success.[1]

In this study, we focused on a class of pharmaceuticals derived from bisphosphonates. Bisphosphonates are commonly used oral medications for the treatment of osteoporosis.[2] The pharmacological function of these active compounds is determined by their P–C–P backbone, where two phosphate groups are covalently linked to a carbon atom. The poor lipophilicity of bisphosphonates limits their absorption from the gastrointestinal tract. The incorporation of hydrophobic side chains into the bisphosphonate structure helps overcome these limitations and offers potential benefits across various therapeutic areas, including cancer and parasitic infections. Thus, a method capable of distinguishing bisphosphonates based on their lipophilicity would be a valuable tool for early-stage physicochemical screening in pharmaceutical research.

The *n*-octanol : water partition coefficient Ko : *w* (*P*) is a measure of lipophilicity in the absence of relevant speciation and refers to the neutral form of a substance. Ko : *w* is defined as the ratio of concentrations in an organic phase, typically *n*-octanol, and an aqueous phase.[3] Various techniques, such as the classical shake-flask method, allow the log *P* of a neutral compound to be measured but, until recently, none was well-adapted to the study of electrically charged species.[4] Recent work has shown that cyclic voltammetry at the interface between two immiscible electrolyte solutions (ITIES) is the method of choice to study the lipophilicity of cations,[5–7] in particular drugs that can be protonated.[8] In contrast, relatively little has been undertaken concerning the hydrophilic behavior of anions.

Polyaniline (PANI) is a polymer whose structure and properties are highly sensitive to synthesis conditions.[9] In particular, the choice of doping acid and the presence of salts during chemical oxidative polymerization can significantly influence the morphology of the resulting PANI and the types or concentrations of dopant ions incorporated. Previous studies have shown that different protonic acids yield PANI with distinct microstructures – for example, PANI doped with small inorganic acids such as HCl tends to form aggregated, granular, or globular structures, whereas larger organic sulfonate dopants favor more fibrous or networked morphologies.[9] The acidity of the reaction medium also plays a crucial role: higher acid concentrations generally increase the extent of protonation and

[a]*Department of Analytical Chemistry, University of Chemistry and Technology, Prague, Technická 5, Prague 6, 166 28, Czech Republic. E-mail: tatiana.shishkanova@vscht.cz*
[b]*Department of Physics and Measurements, University of Chemistry and Technology, Technická 5, Prague 6, 166 28, Czech Republic*

Table 1 Comparison of the proposed potentiometric array with established approaches for bisphosphonate analysis/lipophilicity-related assessment

Criterion	Potentiometric ISM array[24]	Chromatography[25]
Output	Pattern-based discrimination	Quantitative separation + identification/quantification
Time per sample	Minutes; no separation step	Minutes per LC run + instrument overhead
Cost	Low	High
Miniaturization	High potential	Limited
Matrix handling	Demonstrated for dissolved dosage	Established for complex matrices *via* sample prep + MS selectivity

can lead to well-defined globular PANI particles, while milder conditions or the absence of added acid may result in mixed morphologies[10] (*e.g.*, fibers, plates) or smaller aggregates.[11] In addition to acids, inert salts in the polymerization mixture (providing different anions and ionic strengths) have been reported to modulate PANI nanostructure formation by affecting nucleation and growth – for instance, adding NaCl or other salts can alter fiber diameters or modulate aggregation tendencies of PANI.[12] The ordering in PANI is moderated by water intercalation, most probably between the amine nitrogens of the adjacent chains. Apparently, such hydration depends on the type of anions used in PANI synthesis. This capability is certainly related to the ions' solvation specificity. The oxygen-containing anions are notorious for involving more water molecules in their hydration shells than single-atom anions.[9] In PANI-coated PVC membranes, these effects are compounded by the interaction of PANI growth with the substrate surface. Understanding how polymerization conditions like salt anion (Cl^- *vs.* SO_4^{2-}) and the use of an acid dopant influence the surface morphology and elemental composition of PANI-based membranes is important for tailoring their properties (*e.g.*, ionic transport, homogeneity, and functional group content) for applications.

We have recently shown that polyaniline (PANI) as an outer layer on a plasticized PVC membrane surface in a potentiometric sensor promotes the transport of highly hydrated sulfates from the aqueous medium.[13,14] This phenomenon resulted from stronger PANI hydration in the presence of highly hydrated anions, which facilitated their transport through the inter-particle space of the PANI layer.[9] The successful use of the potentiometric sensors, either individually or as part of a sensor array, particularly in real sample analysis, has motivated several research laboratories to pursue their development.[15–18]

In this work, we propose a novel sensor array based on ion-selective membranes (ISMs) coated with PANI layers to discriminate bisphosphonate pharmaceuticals based on their lipophilicity. The subject of our pilot studies was bisphosphonates in oral pharmaceutical preparations (dosage-form matrices) with well-defined composition. A comparative analysis of a series of PANI-coated experimental ISMs, prepared either with or without the anion-exchanger, under varying polymerization conditions, was carried out. The influence of salt anion (Cl^- *vs.* SO_4^{2-}) and acid usage (polymerization with or without added HCl) on the surface morphology (analyzed by scanning electron microscopy, SEM) and elemental composition (from energy-dispersive X-ray spectroscopy, EDS) of the PANI-coated ISMs was examined. By comparing these samples and integrating literature reference data, we aim to clarify how the presence of different anions and the acidity of the polymerization medium affect dopant incorporation (Cl, S, *etc.*), PANI's distribution on the membrane, and the resulting polymer microstructure. Key findings are compared with those in prior reports on PANI doping to provide a deeper understanding and to highlight novel observations. Furthermore, the potentiometric signals recorded from the sensor array were processed using Principal Component Analysis (PCA) to discriminate between bisphosphonates based on their lipophilicity in both standards and commercial samples.

From an analytical perspective, bisphosphonates are notoriously challenging chromatographic analytes due to their strong hydrophilicity and multivalent ionization. Consequently, many reported workflows use derivatization-assisted LC-MS/MS to improve retention and detectability, while more recent approaches increasingly rely on derivatization-free separation modes such as HILIC-MS/MS or ion chromatography coupled to MS/HRMS for sensitive determination in biological and pharmaceutical matrices,[19–22] where sample preparation and matrix effects are often decisive for reliable quantification (Table 1).[23]

In this context, the proposed potentiometric sensor array is intended as a complementary approach enabling rapid, separation-free discrimination of bisphosphonate pharmaceuticals in dissolved dosage-form matrices under application-relevant aqueous conditions.[21,22]

2. Materials and methods

2.1. Chemicals

The ISMs were prepared using PVC, 2-nitrophenyl octyl ether (NPOE), tridodecylmethylammonium chloride (TDDMACl) and tetrahydrofuran (THF) (Fluka, Selectophore, Switzerland). The deposition of the PANI layer onto the surface of PVC-ISMs was carried out from mixtures prepared from aniline hydrochloride (Fluka, Switzerland), ammonium peroxydisulfate (Lachema, Czech Republic) in the medium of hydrochloric acid mixed with either sodium chloride or sodium sulfate (Lachema, Czech Republic). Standard solutions of bisphosphonates were prepared from sodium salts of trihydrate alendronate (TGI, Japan), ibandronate (TGI, Japan), risedronate (Zentiva, Czech Republic), and clodronate (Merck, USA) (Table 2). For highly ionizable bisphosphonates, experimental partitioning is complicated by multiple protonation states; predicted log *P* values should be interpreted cautiously and primarily as comparative descriptors.[26]

Table 2 Structure and lipophilicity of the tested bisphosphonates[a]

Bisphosphonate	Structure	Log *P*	Log *D* pH = 6	Log *D* pH = 9
Clodronate (C)	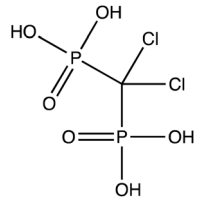	−3.39	−3.83	−4.69
Alendronate (A)	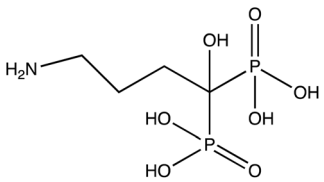	−4.23	−4.52	−5.25
Risedronate (R)	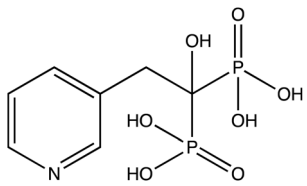	−2.95	−3.95	−4.95
Ibandronate (I)	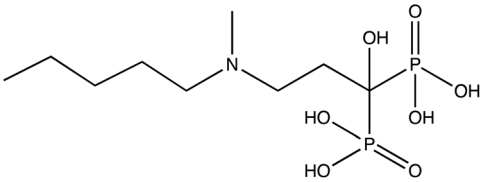	−1.77	−1.49	−2.28

[a] Log *P* and log *D* values are software-predicted descriptors used for comparative interpretation; they were not experimentally determined in this work.

The following commercial bisphosphonates were purchased Ibandronat Mylan, Risendros, Fosavance, Bonefos. Table 3 presents the composition of the commercial bisphosphonate-based pharmaceuticals.

2.2. Instrumentation

The wettability of the surface of the PANI-modified ISMs was measured using a Biolin Scientific Attension Theta Flex instrument (Biolin Scientific, UK) and the results were processed using the OneAttension software. Potentiometric measurements were performed using a pH meter (Labio, pHI 04). The electromotive force (EMF) was measured for the experimental ISE set against a reference silver/silver chloride electrode (Ag/AgCl, 3 mol L^{-1} KCl) (Fig. S1).

The surface morphology of the PANI-modified PVC membranes was analyzed using a MIRA 3 field emission scanning electron microscope (FE-SEM; TESCAN, Brno, Czech Republic) equipped with a secondary electron detector (Everhart–Thornley type). SEM images were captured at various magnifications (up to 100 000×) with an accelerating voltage of 5 kV, allowing qualitative assessment of surface roughness, particulate formations, and coating uniformity. Elemental composition and distribution were assessed using an energy-dispersive X-ray spectrometer Quantax 200 with an XFlash 6 detector (Bruker Nano GmbH, Berlin, Germany). EDS measurements were performed on the membrane surface, with an estimated interaction depth of approximately 400 nm and a lateral interaction radius of about 200 nm. Elemental mapping confirmed the spatial distribution of dopant elements (*e.g.*, Cl, Na, S), while semi-quantitative analysis (% by weight of C, N, O, Na, S, and Cl) was used to compare polymerization conditions.

2.3. Preparation and modification of ion-selective membrane surface

Two compositions of ISMs were used in the present study, namely membranes without (membrane 1) and with an anion-exchanger (membrane 2). Membranes 1 and 2 are uncoated controls (1 = without anion-exchanger, 2 = with TDDMACl), while A–C indicate PANI deposition conditions (A: no added salt; B: NaCl; C: Na_2SO_4). The content of anion-exchanger (TDDMACl) was 1 wt%, the ratio NPOE : PVC was 1 : 2 (wt%) for 0.1 g ISMs. The PVC : NPOE ratio and TDDMACl loading were kept constant using a literature-standard plasticized PVC

Table 3 Composition of commercial bisphosphonate-based pharmaceuticals

Commercial pharmaceuticals	Active substance	Drug content	Excipients
Ibandronat Mylan	Monohydrate sodium ibandronate	150 mg	Lactose monohydrate, povidone, microcrystalline cellulose, crospovidone, colloidal anhydrous silica, magnesium stearate, hyprolose, macrogol, titanium dioxide, shellac, black iron oxide and propylene glycol
Risendros	Sodium risedronate	35 mg	Microcrystalline cellulose, crospovidone, magnesium stearate, hypromellose 2910/5, talc, macrogol 6000, titanium dioxide (E 171), red iron oxide (E 172), yellow iron oxide (E 172)
Fosavance	Trihydrate sodium alendronate	70 mg	Vitamin D3, microcrystalline cellulose (E 460), lactose, medium saturated triacylglycerols, gelatin, croscarmellose sodium, sucrose, colloidal anhydrous silica, magnesium stearate (E 572), butylhydroxytoluene (E 321), modified maize starch and aluminosilicate
Bonefos	Disodium clodronate	300 mg	Microcrystalline cellulose, colloidal anhydrous silica, croscarmellose sodium, stearic acid 95%, magnesium stearate, macrogol 3350, partially hydrolyzed polyvinyl alcohol, talc, titanium dioxide

Table 4 Experimental conditions used at deposition of PANI layer onto the surface of ion-selective membranes

		Polymerization mixture ($V = 10$ mL)			
Active component	Symbol	0.08 mol L^{-1} $(NH_4)_2S_2O_8$	0.08 mol L^{-1} ANI HCl	3.3 mol L^{-1} NaCl	1.0 mol L^{-1} Na_2SO_4
Blank	1	—	—	—	—
	1A	+	+	—	—
	1B	+	+	+	—
	1C	+	+	—	+
TDDMACl (anion-exchanger)	2	—	—	—	—
	2A	+	+	—	—
	2B	+	+	+	—
	2C	+	+	—	+

ISM formulation to ensure comparability across the membrane series.[13,14] The deposition of the PANI-polymeric layer was carried out using the chemical oxidation of aniline hydrochloride (ANI·HCl) with 0.08 mol L^{-1} $(NH_4)_2S_2O_8$ in 1.5 mol L^{-1} HCl at 0 °C for 3 h (Table 4), corresponding to a 1 : 1 molar ratio of oxidant to monomer in the polymerization mixture ($V = 10$ mL), in the presence of the PVC membrane and with or without added inorganic salts. Here, $(NH_4)_2S_2O_8$ acts as the oxidant for aniline polymerization, while HCl provides protonic doping of PANI; the available anions (Cl^-/SO_4^{2-}) determine the counter-ion environment during growth.

After deposition of the PANI-layer, the ISMs were removed from the polymerization mixture, rinsed with 1.5 mol L^{-1} HCl aqueous solution, and treated ultrasonically for 10 min in 1.5 mol L^{-1} HCl aqueous solution.

2.4. Potentiometric measurements and data processing

The potentiometric responses of the experimental ISEs were measured using both standard and commercial bisphosphonate samples. The concentrations of the standard solutions corresponded to those of the respective bisphosphonates in commercial pharmaceutical formulations: c $(A) = 5.9$ mmol L^{-1}, c $(I) = 2.9$ mmol L^{-1}, c $(R) = 1.9$ mmol L^{-1}, c $(C) = 5.5$ mmol L^{-1}. The electrodes were subsequently regenerated for 15 min in 10 mmol L^{-1} NaCl, followed by distilled water. Data processing was performed using principal component analysis (PCA).

3. Results and discussion

3.1. Lipophilicity of ion-selective membranes and bisphosphonates

Contact angle measurements provide information on surface wettability, which reflects the lipophilicity of the surface. The main idea was to adjust the surface lipophilicity of the PVC-ISMs by using different polymerization mixtures to deposit the PANI layer and by varying the membrane composition. Based on contact angle measurements (Table 5), it is evident that the surface wettability/lipophilicity is influenced by both the membrane formulation and the PANI polymerization conditions. Each contact-angle value is reported as mean ± SD from five independent droplets placed at different positions on the membrane surface ($n = 5$).

Table 5 Evaluation of lipophilicity of the surface of the experimental ion-selective membrane after deposition of the PANI-layer ($n = 5$)

	Contact angles, θ°			
Membrane	—	*A*	*B*	*C*
1 (Blank)	89.2 ± 4.9	87.5 ± 3.9	85.1 ± 4.0	53.0 ± 2.1
2 (TDDMACl)	45.3 ± 1.9	44.4 ± 1.8	41.9 ± 1.9	29.0 ± 2.3

The addition of Na_2SO_4 to the polymerization mixture resulted in lower contact angles (membranes 1C and 2C). Minor deviations in contact angles for ISMs based on TDDMACl and modified under similar conditions indicate good reproducibility of the PANI-layer coating on their surfaces.

According to the calculated distribution coefficients (log *D*), the lipophilicity of bisphosphonates followed the order: clodronate (−4.69) < alendronate (−4.52) < risedronate (−3.95) < ibandronate (−1.49) (Table 2). A higher log *D* value corresponds to a more lipophilic substance. Among the bisphosphonates, ibandronate is the most lipophilic one. The lipophilicity of clodronate and risedronate is similar.

3.2. SEM and EDS analysis

The surface morphology and elemental composition of ISMs coated with PANI were investigated using SEM and EDS. To optimize composition, we fixed the bulk membrane formulation and systematically varied only the PANI deposition conditions (A–C) to isolate the role of the surface layer. These analyses revealed significant differences in the structure and uniformity of the PANI layers, which were strongly influenced by the composition of the underlying membrane, the form of the aniline monomer, and the anion of salt (Cl^- *vs.* SO_4^{2-}) present during polymerization. Salt ions present during oxidative polymerization are known to markedly affect PANI microstructure and ordering, including fibrillar/ordered morphologies and crystallinity, through coupled effects on chain growth, counterion interactions, and water organization during film formation.[9]

Unmodified blank (PVC : NPOE) membranes exhibited a relatively smooth and featureless surface at the microscale, whereas PANI-coated membranes showed enhanced surface roughness and morphological diversity depending on the polymerization conditions.

The influence of TDDMACl on PANI morphology was investigated using samples 1A and 2A. As illustrated in Fig. 1 and S2, comparison of samples 1A (PVC : NPOE without TDDMACl) and 2A (PVC : NPOE with TDDMACl) highlights the pronounced effect of membrane composition on PANI morphology. Sample 1A exhibited irregular spherical or globular PANI formations, while sample 2A displayed a more compact layer, indicating improved layer formation. The presence of the anion-exchanger (TDDMACl) in the 2A sample likely facilitated PANI nucleation and promoted a more uniform distribution of the polymer. EDS spectra (Table 6) supported these observations, showing elevated nitrogen and chlorine signals in 2A, confirming successful PANI deposition and effective Cl doping. In addition, trace signals of sulfur in sample 1A may indicate the presence of residual oxidant $(NH_4)_2S_2O_8$ that may remain embedded within the polymer layer.

The influence of salt anion on PANI morphology was evaluated using membranes 2A, 2B, and 2C, which shared the same PVC : NPOE : TDDMACl composition and were coated with PANI with differing salt additions in the polymerization mixture (Table 4). As shown in Fig. 2 and S3, sample 2A (no added salt) exhibited only partial PANI surface coverage, with small, spherical aggregates sparsely distributed across the membrane.

In contrast, sample 2B, PANI deposited in the presence of NaCl, revealed a denser, more homogeneous granular morphology, with numerous packed clusters of PANI nodules and increased surface roughness. This suggests that the addition of NaCl, promoting chloride doping, enhances polymer nucleation and particle aggregation. EDS analysis confirmed elevated Cl content in sample 2B, indicating effective dopant incorporation and a thicker PANI layer. Sample 2C, PANI deposited in the presence of Na_2SO_4, displayed a distinctly different morphology characterized by a fine, more uniform layer with dispersed microstructures and crystalline domains. Compared with chloride-doped coatings, sulfate-doped PANI exhibited reduced clustering and a more evenly distributed morphology, likely due to altered nucleation kinetics in the presence of sulfate ions. Because sulfate is strongly hydrated and measurably reshapes water hydrogen-bonding, it can alter local solvation and nucleation/growth during PANI formation, leading to more uniform morphologies.[27,28] These results underscore the critical role of salt and dopant anion type in shaping the final architecture of the PANI layer.

To evaluate the effect of monomer form on PANI morphology, samples 2B (aniline hydrochloride) and 2B* (aniline base with an equimolar amount of added HCl), both polymerized in the presence of NaCl, were compared (Fig. 3 and S4). Both the PANI-coated surfaces exhibited polymer layers with high surface roughness and comparable structures. Only subtle morphological differences were observed, suggesting that the initial monomer form had limited influence on the overall surface appearance. However, EDS analysis revealed lower chlorine and nitrogen signals in 2B*, which may reflect a reduced degree of Cl doping or PANI incorporation compared to 2B.

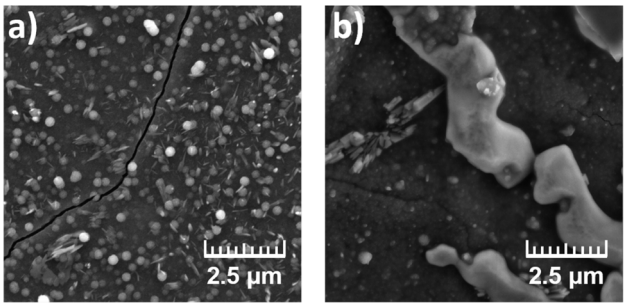

Fig. 1 SEM micrographs of PANI-coated (a) blank (1A) and (b) TDDMACl-based (2A) membranes.

Table 6 Normalized EDS elemental composition (weight %) of the PANI-coated membranes *vs.* reference

Active component	Symbol	C (wt%)	N (wt%)	O (wt%)	Na (wt%)	S (wt%)	Cl (wt%)
Blank	1	84.92 ± 9.94	6.11 ± 1.35	7.72 ± 1.37	0.98 ± 0.08	0.07 ± 0.03	0.20 ± 0.04
	1A	53.56 ± 4.63	7.00 ± 0.89	14.76 ± 1.48	5.84 ± 0.26	4.16 ± 0.17	14.69 ± 0.58
	1B	68.42 ± 6.29	8.57 ± 1.13	5.93 ± 0.75	0.12 ± 0.03	0.33 ± 0.04	16.62 ± 0.72
	1C	67.10 ± 6.89	10.60 ± 1.51	6.96 ± 0.96	0.35 ± 0.04	0.35 ± 0.04	14.65 ± 0.70
TDDMACl (anion-exchanger)	2	83.75 ± 9.41	2.58 ± 0.59	5.78 ± 0.93	0.05 ± 0.03	0.00 ± 0.00	7.84 ± 0.43
	2A	69.09 ± 6.12	7.76 ± 1.04	5.55 ± 0.71	0.00 ± 0.00	0.48 ± 0.04	17.13 ± 0.70
	2B	62.38 ± 4.32	8.31 ± 0.88	3.01 ± 0.36	2.58 ± 0.11	0.00 ± 0.00	23.72 ± 0.73
	2B*	69.56 ± 6.71	7.87 ± 1.11	4.82 ± 0.67	2.03 ± 0.12	0.00 ± 0.00	15.72 ± 0.72
	2C	63.56 ± 5.07	8.07 ± 0.94	7.46 ± 0.79	3.06 ± 0.14	1.43 ± 0.07	16.41 ± 0.60

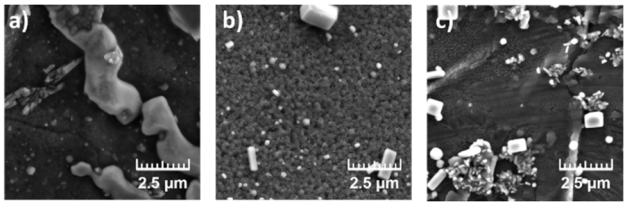

Fig. 2 SEM micrographs of PANI-coated membranes based on an anion exchanger (TDDMACl) and prepared with different salts in the polymerization mixture. (a) Sample 2A (no added salt) shows a more compact and uniform structure. (b) Sample 2B (with NaCl) exhibits a morphology with high roughness. (c) Sample 2C (with Na_2SO_4) displays a heterogeneous surface with finer dispersed features, indicating altered nucleation behavior due to sulfate doping.

Overall, the morphology of PANI coatings was strongly influenced by both the membrane composition and polymerization conditions. The incorporation of TDDMACl into the membrane matrix promoted more uniform PANI coverage, while the addition of NaCl in the polymerization mixture enhanced surface roughness due to improved nucleation and dopant incorporation. Substitution of NaCl with Na_2SO_4 yielded smoother coatings with finer features, suggesting altered nucleation behavior under sulfate doping. Although the monomer form (aniline base *vs.* aniline hydrochloride) had only a subtle impact on surface morphology, EDS confirmed reduced nitrogen and chlorine content when aniline base was used,

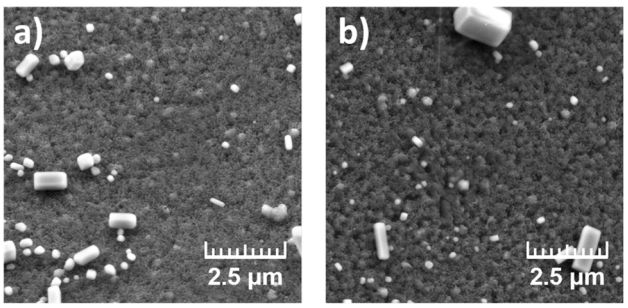

Fig. 3 SEM images showing the effect of monomer form on the morphology of PANI-layer on the membrane surface. (a) Sample 2B* (aniline base + NaCl) and (b) sample 2B (aniline hydrochloride + NaCl) both exhibit granular polymer structures with high surface roughness. Only subtle morphological differences are visible.

implying lower PANI incorporation or doping efficiency. Together, these results highlight how small variations in membrane formulation and polymerization chemistry can be used to tailor the microstructure and surface properties of PANI-based membranes.

Table 6 summarizes the normalized weight percentage of key elements (C, N, O, Na, S, Cl) detected by EDS on the surface of the reference membrane and the PANI-coated samples prepared under different conditions. The reference blank (PVC : NPOE) membrane is composed primarily of carbon, oxygen and nitrogen and shows only minor traces of other elements. In contrast, all PANI-coated samples exhibit significant dopant-related elements (Cl, and in some cases Na and S), confirming the presence of the PANI polymer and the incorporation of the doping anions from the reaction medium.

By elemental composition, carbon (C) is the most abundant element, followed by nitrogen (N), oxygen (O) and sulfur (S), consistent with the literature data concerning the composition of PANI coatings prepared through chemical polymerization.[29] The carbon content decreased across the PANI-coated membranes (53.6–69.6 wt%) compared to the reference (84.9 wt%), likely due to accumulation of inorganic residues on the surface. The lowest carbon content was observed in sample 1A.

All PANI-coated samples exhibited elevated nitrogen content (approx. 7.0–10.6 wt%) present in the aniline monomer units compared to the reference (approx. 6.1 wt%), confirming successful PANI deposition. An unusually high oxygen content (14.8 wt%), along with elevated Na (5.8 wt%) and S (4.2 wt%) was found in sample 1A (no added salt), likely due to residual oxidant or sulfate salt retained on the layer. Other samples had moderate O levels (approx. 3.0–7.7 wt%), likely from the underlying membrane or oxidant by-products.

Chlorine levels were markedly higher in samples 1B (16.6%) and 2B (23.7%) both modified in the presence of NaCl, indicating substantial retention of chloride species, further enhanced by the anion-exchanger TDDMACl. Samples deposited in the presence of Na_2SO_4 (1C: 0.4 wt% and 2C: 1.4 wt%) showed higher sulfur content compared to the uncoated samples (Sample 1: 0.1 wt% and Sample 2: 0.0 wt%). Better-hydrated anions, such as sulfates, can provide more efficient hydration of the amine nitrogens of the PANI chains and, consequently, improve incorporation/doping through the PANI layer.[13] In conclusion, EDS confirmed that both the choice of

dopant and polymerization conditions significantly affect the elemental composition of the PANI layers.

3.3. Potentiometric measurements

To achieve selective discrimination among pharmaceuticals differing in lipophilicity, the PANI layer was deposited using various procedures, including the addition of different inorganic salts to the polymerization mixture. Scheme 1 illustrates the proposed roles of the hydrated PANI surface region and dopant/counterion environment in modulating access and partitioning of charged analyte species at the sensing interface.

The potentiometric experiments were carried out at pH 5.5, mimicking the typical pH of dissolved bisphosphonate formulations. A pH of 5.5 was selected because it reduces esophageal irritation caused by oral bisphosphonates. PANI is known to exhibit pH-dependent redox activity. However, in our system, the PANI layer primarily acts as a surface-modifying ion-exchanger rather than a redox-active material (Fig. S5 and S6). For the pH-dependence experiment, ISMs with different surface properties and varying active components, namely 1B, 1C (blank, without ion-exchanger), and 2, 2A, 2B, 2C (with ion-exchanger) were selected. The concentration of bisphosphonate solutions corresponded to those in commercial pharmaceuticals. Obviously, the contact of the ISMs in the sensor array with bisphosphonates causes an ion-exchange process at the phase boundary between the sample and PANI-modified surface. Table S1 presents the main potentiometric properties of the tested ISMs towards studied bisphosphonates and highlights the effect of the deposited PANI layer. The PANI-coated analogues (1A–1C and 2 A–2C) exhibit altered potentiometric signals and improved discrimination between bisphosphonates (Fig. S7). These findings are consistent with the role of PANI as a functional interfacial layer whose morphology and dopant incorporation depend on polymerization conditions. Hydration-driven solute exclusion/partitioning near polymer surfaces can be governed by short-range water structuring forces with Hofmeister-type ion specificity, highlighting why modifying a hydrophobic membrane interface with a hydrated PANI layer can alter ion/solute access and transport.

To ensure operation and reproducible results obtained from the sensor array, a regeneration procedure was implemented as follows. Between a series of repeated measurements, the ISMs

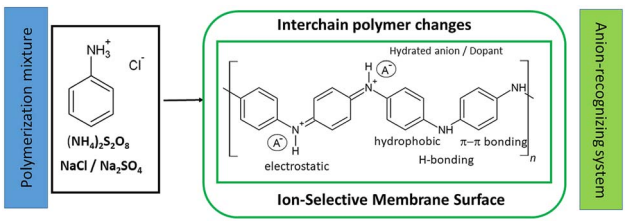

Scheme 1 Conceptual illustration of PANI deposition on an ion-selective membrane surface. Oxidative polymerization of aniline (APS, $NaCl/Na_2SO_4$) yields protonated PANI (emeraldine salt) with counter-anion (A^-), where the dopant anion environment influences interchain interactions and the resulting anion-recognizing surface.

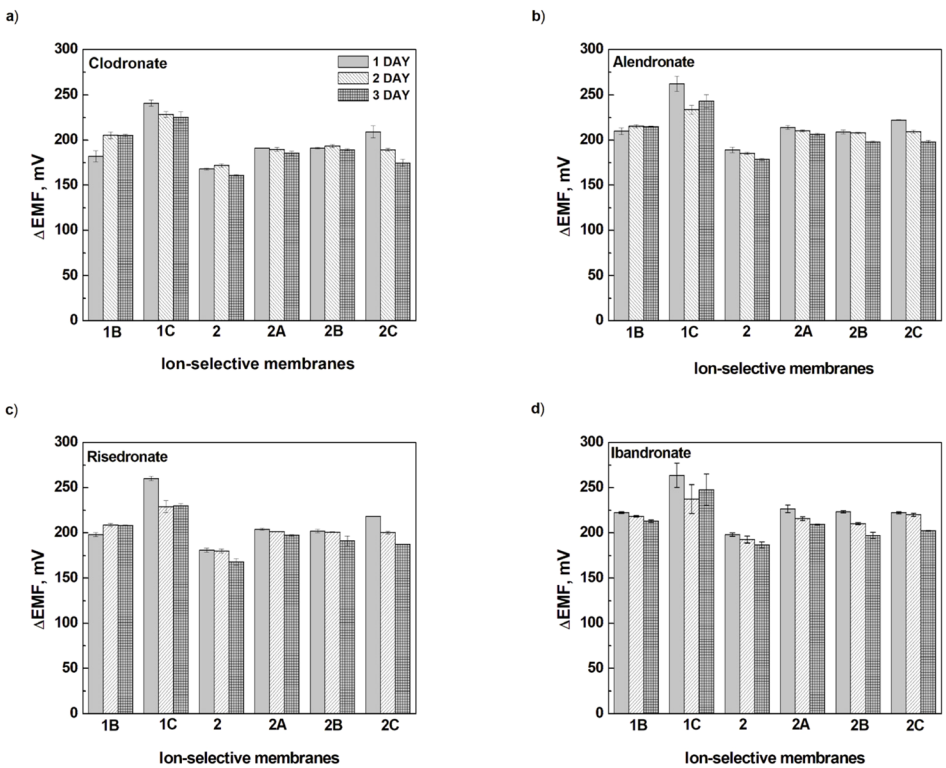

Fig. 4 Potentiometric signals of experimental PANI-modified membranes towards bisphosphonate pharmaceuticals in time (n = 5): (a) clordronate (Bonefos), (b) alendronate (Fosavance), (c) risedronate (Risendros) and (d) ibandronate (Ibandronat Mylan). Note: exemplary raw data of potentiometric signals (mV *vs.* time) are Fig. S6. Processed data present herein are in Table S1.

were washed with 1.0 mmol L^{-1} NaCl solution. The concentration of the regeneration solution was selected to be high enough to allow such recovery for a short time, but not so high as to mask the ions' response in the sample.

In the next step, the potentiometric responses of the prepared ISMs were measured and their signal stability over time was evaluated (Fig. 4 and Table S2). It was found that the stability of the potentiometric signal was affected by both the composition of the ISM/PANI-layer and the kind of measured bisphosphonate. The lowest RSD values measured over 3 days were obtained for ISM based on an anion exchanger: clodronate (0.4–1.1%), alendronate (0.3–1.3%), risedronate (0.1–1.0%), and ibandronate (0.2–1.5%).

For ISMs based on an anion-exchanger, the PANI layer deposited in the absence (membrane 2A) and the presence of NaCl (membrane 2B) stabilized the potentiometric signal to bisphosphonates, achieving the value $\log D < -1.49$ (namely, clodronate, alendronate, risedronate). It should be noted that the stabilized effect on the potentiometric response was also observed for blank ISMs coated with PANI-layer in the presence of NaCl (membrane 1B), despite the absence of an anion-exchanger. The PANI layer formed under these conditions (1B) is probably relatively thick, potentially enhancing ion-exchange capacity. The observed improvement may be explained by a combination of factors, in particular the properties of the deposited PANI layer (ion-exchange properties, quality, and composition) and the tested bisphosphonate (structure and lipophilicity).

Recently, it has been noted that the anion transport through hydrated PANI depends on its hydration and is influenced by the structure of the anions in the surrounding aqueous medium. Better-hydrated anions with stronger water-structure-perturbing capacity can provide more efficient hydration of the amine nitrogens of the PANI chains and, therefore, improve water permeability through the PANI layer.[13] Comparison of the potentiometric signals of blank ISMs coated with the PANI layer prepared in the presence of Na_2SO_4 (membrane 1C) showed the effect of the lipophilicity of bisphosphonate. A more reproducible signal was obtained with a more hydrophilic bisphosphonate (clodronate, $\log D = -4.69$), which can hydrate the PANI chains.

3.4. Bisphosphonate discrimination

The experimental sensor array consisted of 6 electrodes including the uncoated reference membrane 2 and PANI-modified membranes: 1B, 1C, 2A, 2B, and 2C. It was used to discriminate between bisphosphonates differing in lipophilicity (Table 2). Because bisphosphonates are highly polar and multiply ionized under the measurement conditions, the array response is explained by a synergy of (i) ion exchange within the ISM and (ii) hydration-controlled interfacial transport within the PANI-modified surface region. The PANI layer acts as a functional hydrated interface whose morphology and counter-ion environment depend on polymerization conditions (Cl^- *vs.* SO_4^{2-}), thereby modulating access of charged bisphosphonate species and producing distinct multivariate response patterns. Because the present work is based on a potentiometric array and pattern recognition, performance gains are primarily evaluated through the repeatability of potential patterns and chemometric discrimination, rather than a single sensor parameter. The pure bisphosphonates were tested as standards, and commercial formulations were also tested for comparison (Table 2). The potentiometric responses of the sensor array were processed using Principal Component Analysis (PCA), a multivariate technique commonly used for dimensionality reduction and pattern recognition in sensor data analysis.[30] Here, the first two principal components (PC-1 and PC-2) were retained for interpretation, as they capture the largest portion of the data's variance (Fig. 5 and 6).

All bisphosphonate standards formed distinct clusters, indicating differences in lipophilicity between individual compounds. The PC-1 and PC-2 describe 91% and 6% of variability, respectively (Fig. 5). The variability PC-1 that is responsible for the separation is predominantly influenced by the response of ISMs 1C ($\theta = 53.0°$), 2 ($\theta = 45.3°$), 2A ($\theta = 44.4°$), and 2B ($\theta = 41.9°$). In the case of the PC-2, an important contribution is observed from ISM 1B ($\theta = 85.1°$). The potentiometric signal of a membrane should be regulated by the ion-exchange reaction occurring on the phase boundary membrane/solution. It is possible to propose that the observed separation results from a combination of both the surface properties of ISM and the concentration of ion-exchange sites in the PANI layer. The ion-exchange sites are provided by TDDMACl as an active component in the membrane matrix and chloride as a dopant of the PANI layer. A higher content of exchangeable chloride was determined in the PANI layer of ISMs 1C (Cl: 14.6 wt%), 2A (Cl: 17.1 wt%), and 2B (Cl: 23.7 wt%), which influenced PC-1. In the case of 1B ISM, the PANI layer showed a high chloride content (16.6 wt%), but its insufficient hydrophilicity ($\theta = 85.1°$) may explain its limited contribution to bisphosphonate discrimination.

Further, the experimental sensor array was used to differentiate commercial bisphosphonate-based pharmaceuticals, as a test of matrix selectivity (Table 2 and Fig. 6). Commercial tablet formulations inherently contain common excipients (*e.g.*, fillers, binders, disintegrants, and lubricants). Molecular modeling of hydrated PANI supports the presence of structured hydrogen-bonding around PANI nitrogen sites and indicates that counterions (*e.g.*, Cl^-) can remain highly solvated, consistent with hydration-controlled ion association at the PANI/water interface.[28] From a mechanistic viewpoint, the array response is dominated by interactions among charged bisphosphonate species, the membrane anion-exchanger, and the surface region (including adsorption effects). Therefore, the most plausible interferents in dissolved dosage forms are competing ions (*e.g.*, chloride, sulfate, phosphate, carbonate, citrate, stearate, croscarmellose, Fig. S8) and, in general, species capable of adsorption at the sensing interface. In contrast, many standard excipients are neutral polymers or poorly soluble solids and are expected to have limited direct contribution to the potentiometric pattern after dissolution. According to PC-1, pharmaceuticals containing less and more lipophilic bisphosphonates, namely clodronate ($\log D = -4.69$) and ibandronate ($\log D =$

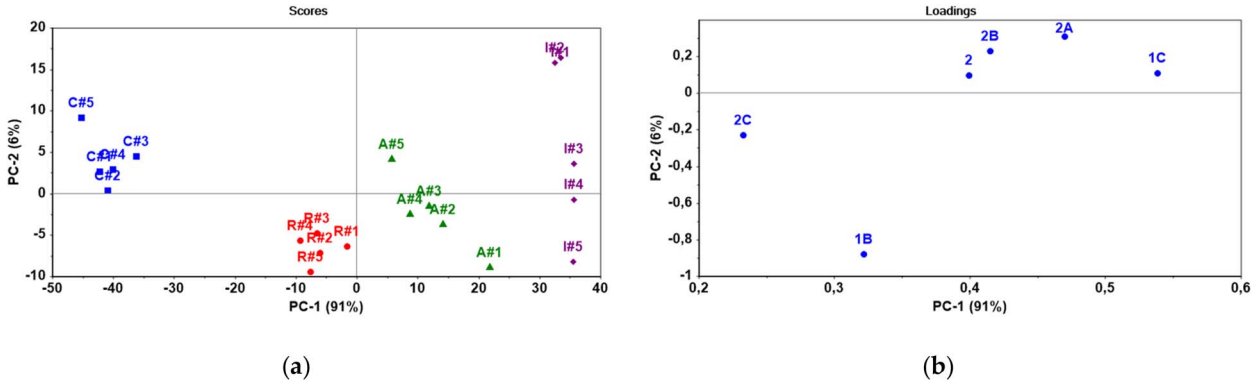

Fig. 5 (a) PCA score plot: discrimination between bisphosphonate standards: clodronate (C), alendronate (A), risedronate (R), and ibandronate (I). (b) PCA loading plot for the sensor array when analyzing the pharmaceutical samples.

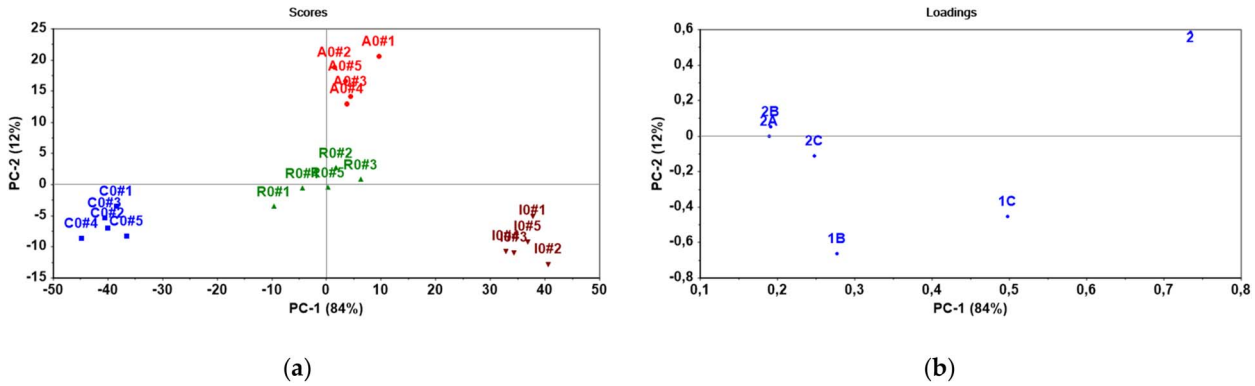

Fig. 6 (a) PCA score plot: discrimination between commercial pharmaceuticals derived from bisphosphonates: clodronate (C), alendronate (A), risedronate (R), and ibandronate (I). (b) PCA loading plot for the sensor array when analyzing the pharmaceutical samples.

−1.49) differ significantly, which is in the agreement with the signal patterns obtained for their standards (Fig. 5a and 6a). As can be seen from Fig. 6a, risedronate ($\log D = -3.95$) occupied an intermediate position between less lipophilic clodronate ($\log D = -4.69$) and more lipophilic ibandronate ($\log D = -1.49$). From the perspective of PC-1 (84% of variability), a considerable effect is observed from ISMs 2 ($\theta = 45.3°$) and 1C ($\theta = 53.0°$), while a weaker effect is from other ISMs: 2A ($\theta = 44.4°$), 2B ($\theta = 41.9°$) and 2C ($\theta = 29.0°$). We can assume that a selected combination of ISMs is suitable to distinguish the lipophilic bisphosphonates in a real matrix. Despite these constituents, PCA models correctly classified all commercial preparations during cross-validation (Fig. 6), indicating that typical dosage-form components do not compromise the array's discrimination capability under the applied measurement conditions.

As shown in Fig. 5 and 6, the PCA score plots clearly show that the potentiometric sensor array differentiated bisphosphonates in both cases, indicating that the presence of matrix components in commercial products did not prevent successful classification. To better illustrate the results, the data were also presented with a PCA-LDA plot using 5 factors (Fig. S9, S10 and Tables S3, S4). As is apparent, the total cross-validation (leave-one-out, full-cross) provides 100% accuracy of sample classification. This is illustrated by the confusion matrices (Tables S3 and S4), where the positions of the actual and predicted values fully overlap.

4. Conclusions

This study presents a systematic investigation of how membrane composition, dopant type, and monomer form influence the surface morphology and elemental composition of PANI coatings on PVC : NPOE-based ISMs. Through combined SEM and EDS analyses, we demonstrated that both the presence of the cationic additive TDDMACl and the specific deposition conditions, including the type of salt anion, play a critical role in determining the structure and chemical properties of the resulting PANI layers.

Three principal trends in surface morphology were observed. First, the inclusion of TDDMACl anion exchanger in the membrane modified PANI layer, producing more uniform coating compared to membranes without TDDMACl, which showed globular aggregates. Second, the type of salt used during deposition had a clear impact: NaCl promoted the formation of thick layers with high surface roughness and elevated chlorine content, while Na_2SO_4 led to finer, more homogeneous layers with detectable sulfur incorporation.

Third, deposition with aniline base, rather than fully protonated aniline hydrochloride, resulted in comparable overall roughness but subtle morphological differences.

In conclusion, the interplay between membrane formulation (PVC : NPOE *vs.* PVC : NPOE : TDDMACl), dopant type (Cl^- *vs.* SO_4^{2-}), and monomer form (aniline or aniline hydrochloride) allows for controlled tuning of PANI layer morphology and composition. These structural differences are expected to influence functional performance. To demonstrate the analytical utility of these modifications, a potentiometric sensor array comprising PANI-modified ISMs was used to classify bisphosphonates differing in lipophilicity. Principal component analysis of the sensor responses revealed that electrodes with distinct membrane morphologies and compositions contributed differentially to the discrimination of both standard and commercial bisphosphonates. In particular, PC1 correlated with bisphosphonate lipophilicity, showing clear discrimination and supporting the potential of membrane engineering for enhanced chemical sensing. The proposed approach can be a valuable tool for rapid discrimination of drugs based on their lipophilicity.

Future work could build on these findings by examining how these morphological and compositional differences translate to performance metrics (*e.g.*, ion transport, sensor response) and by exploring other dopants or polymerization methods to further tailor PANI-based membranes.

Author contributions

Conceptualization, T. V. S.; methodology, T. V. S.; investigation, A. S. C. and J. O.; resources, T. V. S and M. V.; data curation, T. V. S., A. S. C., J. O. and M. Č.; writing–original draft preparation, T. V. S. and J. O.; writing–review and editing, T. V. S., J. O.; visualization, T. V. S., J. O. and M. Č.; supervision, T. V. S.; project administration, M. V.; funding acquisition, T. V. S. and M. V.

Conflicts of interest

There are no conflicts to declare.

Data availability

Supplementary information (SI): Fig. S1: Schematic of experimental array used in the present work; Fig. S2: SEM images at 100 000× magnification of PANI-coated membranes (a) blank (1A) and (b) TDDMACl-based (2A); Fig. S3: SEM micrographs at 100 000× magnification of PANI-coated membranes based on an anion exchanger (TDDMACl), prepared with different salts in the polymerization mixture: (a) Sample 2A (no added salt) shows a more compact and uniform structure. (b) Sample 2B (with NaCl) exhibits a morphology with high surface roughness. (c) Sample 2C (with Na_2SO_4) displays a heterogeneous surface with finer dispersed features, indicating altered nucleation behavior due to sulfate doping; Fig. S4: SEM images at 100 000× magnification showing the effect of monomer form on the morphology of the PANI layer on the membrane surface. (a) Sample 2B* (aniline base + NaCl) and (b) Sample 2B (aniline hydrochloride + NaCl) both exhibit granular polymer structures with high surface roughness. Only subtle morphological differences are visible; Fig. S5: pH dependence of experimental membranes prepared in this study and used in the sensor array; Fig. S6: Potentiometric signal of experimental membranes towards ibandronate recorded in time with the sensor array used in the present study; Fig. S7: Potentiometric response of PANI-coated experimental ion-selective membranes prepared without (membrane 1) and with (membrane 2) the anion-exchanger to tested bisphosphonates; Fig. S8: Influence of possible inorganic interferents on the potentiometric selectivity of unmodified and PANI-modified ion-selective membrane based on anion-exchanger; Fig. S9: LDA discrimination chart (sample distance to individual models) for model samples; Fig. S10: LDA discrimination chart (sample distance to individual models) for real samples; Table S1: Potentiometric parameters of experimental ion-selective membranes prepared without (membrane 1) and with (membrane 2) the anion-exchanger modified by the PANI layer towards tested bisphosphonates ($n = 3$); Table S2: Potentiometric signals of experimental PANI-modified membranes towards tested bisphosphonates in time ($n = 5$); Table S3: Confusion matrix obtained by PCA-LDA method for model samples; Table S4: Confusion matrix obtained by PCA-LDA method for real samples. The data supporting this article are available in Zenodo at DOI: https://doi.org/10.5281/zenodo.18429620. See DOI: https://doi.org/10.1039/d5ay01639h.

Acknowledgements

The authors acknowledge funding from Institutional Resources (Department of Analytical Chemistry, UCT Prague, CZ; Grant Number: 402850061). This work has been funded by a grant from the Programme Johannes Amos Comenius under the Ministry of Education, Youth and Sports of the Czech Republic SENDISO project no. CZ.02.01.01/00/22_008/0004596. As set out in the Legal Act, beneficiaries must ensure that the open access to the published version or the final peer-reviewed manuscript accepted for publication is provided immediately after the date of publication *via* a trusted repository under the latest available version of the Creative Commons Attribution International Public Licence (CC BY) or a licence with equivalent rights. For long-text formats, CC BY-NC, CC BY-ND, CC BY-NC-ND or equivalent licenses could be applied. We thank Zentiva for providing bisphosphonates used in this study and for their contribution in bisphosphonate projects.

References

1 J. A. Arnott and S. L. Planey, *Expert Opin. Drug Discovery*, 2012, **7**(10), 863–875, DOI: 10.1517/17460441.2012.714363.
2 N. B. Watts and D. L. Diab, *J. Clin. Endocrinol. Metab.*, 2010, **95**(4), 1555–1565, DOI: 10.1210/jc.2009-1947.
3 J. Quancard, A. Bach, C. Borsari, R. Craft, C. Gnamm, S. M. Guéret, I. V. Hartung, H. F. Koolman, S. Laufer, S. Lepri, J. Messinger, K. Ritter, G. Sbardella, A. U. Lopez,

M. K. Willwacher, B. Cox and R. J. Young, *ChemMedChem*, 2025, **20**(8), e202400931, DOI: 10.1002/cmdc.202400931.
4 G. Bouchard, P.-A. Carrupt, B. Testa, V. Gobry and H. H. Girault, *Pharm. Res.*, 2001, **18**, 702–708, DOI: 10.1023/a:1019846125723.
5 Z. Samec, V. Marecek, J. Koryta and M. W. Khalil, *J. Electroanal. Chem. Interfacial Electrochem.*, 1977, **83**, 393–397, DOI: 10.1016/S0022-0728(77)80186-1.
6 K. Kontturi and L. Murtomaki, *J. Pharm. Sci.*, 1992, **81**, 970–975, DOI: 10.1002/jps.2600811003.
7 G. Caron, G. Steyaert, A. Pagliara, P. Crivori, P. Gaillard, P.-A. Carrupt, A. Avdeef, K. J. Box, H. H. Girault and B. Testa, *Helv. Chim. Acta*, 1999, **82**, 1211–1222, DOI: 10.1002/(SICI)1522-2675(19990804)82:8<1211::AID-HLCA1211>3.0.CO;2-K.
8 F. Reymond, P.-A. Carrupt, B. Testa and H. H. Girault, *Chem. - Eur. J.*, 1999, **5**, 39–47, DOI: 10.1002/(SICI)1521-3765(19990104)5:1<39::AID-CHEM39>3.0.CO;2-3.
9 N. P. Gospodinova, D. A. Ivanov, D. V. Anokhin, I. Mihai, L. Vidal, S. Brun, J. Romanova and A. Tadjer, *Macromol. Rapid Commun.*, 2009, **30**, 29–33, DOI: 10.1002/marc.200800434.
10 S. Golba, M. Popczyk, S. Miga, J. Jurek-Suliga, M. Zubko, J. Kubisztal and K. Balin, *Materials*, 2020, **13**, 5108, DOI: 10.3390/ma13225108.
11 D. O. Ahmat, Z. A. Jawad, V. Khosravi and S. P. Yeap, *J. Phys. Sci.*, 2023, **34**(3), 67–79, DOI: 10.21315/jps2023.34.3.5.
12 R. Wang and Y. Jing, *Des. Monomers Polym.*, 2023, **26**(1), 45–53, DOI: 10.1080/15685551.2023.2166727.
13 T. V. Shishkanova, D. Sykora, H. Vinsova, V. Kral, I. Mihai and N. P. Gospodinova, *Electroanalysis*, 2009, **21**(17–18), 2010–2013, DOI: 10.1002/elan.200904632.
14 T. V. Shishkanova, K. Řezanková and P. Řezanka, *Chem. Pap.*, 2017, **71**(2), 489–494, DOI: 10.1007/s11696-016-0067-6.
15 V. K. Gupta, N. Arunima, B. Singhal and S. Agarwal, *Comb. Chem. High Throughput Screening*, 2011, **14**(4), 284–302, DOI: 10.2174/138620711795222437.
16 T. V. Shishkanova, K. Videnská, S. G. Antonova, M. Kronďák, P. Fitl, D. Kopecký, M. Vrňata and V. Král, *Electrochim. Acta*, 2014, **115**, 553–558, DOI: 10.1016/j.electacta.2013.10.214.
17 O. Özbek, C. Berkel and Ö. Isildak, *Crit. Rev. Anal. Chem.*, 2022, **52**(4), 768–779, DOI: 10.1080/10408347.2020.1825065.
18 P. Ciosek-Skibińska, K. Cal, D. Zakowiecki and J. Lenik, *Materials*, 2024, **17**(20), 5016, DOI: 10.3390/ma17205016.
19 H.-X. Zhang, Y. Li, Z. Li, Ch. W. K. Lam, H.-W. Chen, W.-D. Luo, C.-Y. Wang, Z.-H. Jiang, Z.-Y. Du and W. Zhang, *J. Pharm. Biomed. Anal.*, 2020, **190**, 113579, DOI: 10.1016/j.jpba.2020.113579.
20 Y.-F. Shieh, F.-M. Hung, S.-N. Yeh, L.-T. Kao, J.-C. Chen, F.-E. Liao, J. Huang, C.-H. Wang, C.-Y. Lee and J. Shiea, *J. Pharm. Biomed. Anal.*, 2024, **237**, 115775, DOI: 10.1016/j.jpba.2023.115775.
21 A. S. Y. Wong, B. P.-N. Yuen, C. O. L. Wong, F. K.-W. Kong, Y.-M. So, W. H. Kwok, L. Brooks, T. S. M. Wan and E. N.-M. Ho, *Drug Test. Anal.*, 2025, **17**(4), 506–516, DOI: 10.1002/dta.3753.
22 N. Manousi, P. D. Tzanavaras and C. K. Zacharis, *J. Pharm. Biomed. Anal.*, 2022, **219**, 114921, DOI: 10.1016/j.jpba.2022.114921.
23 J. Klingberg, S. Richards, T. Hochwallner, L. Kennan and J. Keledjian, *Drug Test. Anal.*, 2025, **17**, 997–1001, DOI: 10.1002/dta.3800.
24 R. B. Belugina, Y. B. Monakhova, E. Rubtsova, A. Becht, C. Schollmayer, U. Holzgrabe, A. V. Legin and D. O. Kirsanov, *J. Pharm. Biomed. Anal.*, 2020, **188**, 113457, DOI: 10.1016/j.jpba.2020.113457.
25 A. Port, M. Bordas, R. Enrech, R. Pascual, M. Rosés, C. Ràfols, X. Subirats and E. Bosch, *Eur. J. Pharm. Sci.*, 2018, **122**, 331–340, DOI: 10.1016/j.ejps.2018.07.010.
26 J. Biernacka, K. Betlejewska-Kielak, E. Kłosińska-Szmurło, F. A. Pluciński and A. P. Mazurek, *Acta Pol. Pharm.*, 2013, **70**(5), 877–882.
27 C. P. Lamas, C. Vega and P. Gallo, *Mol. Phys.*, 2024, **122**, 21–22, DOI: 10.1080/00268976.2024.2406260.
28 A. Ivanova, G. Madjarova, A. Tadjer and N. Gospodinova, *Int. J. Quantum Chem.*, 2006, **106**, 1383–1395, DOI: 10.1002/qua.20896.
29 P. B. Anand, K. Hasna, K. M. Anilkumar and S. Jayalekshmi, *Polym. Int.*, 2012, **61**(12), 1733–1738, DOI: 10.1002/pi.4262.
30 P. Ciosek and W. Wróblewski, *Analyst*, 2007, **132**, 963–978, DOI: 10.1039/B705107G.